JOURNAL OF BACTERIOLOGY, Aug. 2003, p. 4345–4353 Vol. 185, No. 15
0021-9193/03/$08.00+0 DOI: 10.1128/JB.185.15.4345–4353.2003

Gene Expression Analysis of Energy Metabolism Mutants of *Desulfovibrio vulgaris* Hildenborough Indicates an Important Role for Alcohol Dehydrogenase

Shelley A. Haveman,[1] Véronique Brunelle,[1] Johanna K. Voordouw,[1] Gerrit Voordouw,[1]* John F. Heidelberg,[2] and Ralf Rabus[3]

Department of Biological Sciences, University of Calgary, Calgary, Alberta, T2N 1N4, Canada[1]; The Institute for Genomic Research, Rockville, Maryland, 20850[2]; and Max-Planck Institute for Marine Microbiology, D-28359 Bremen, Germany[3]

Received 26 February 2003/Accepted 13 May 2003

Comparison of the proteomes of the wild-type and Fe-only hydrogenase mutant strains of *Desulfovibrio vulgaris* Hildenborough, grown in lactate-sulfate (LS) medium, indicated the near absence of open reading frame 2977 (ORF2977)-coded alcohol dehydrogenase in the *hyd* mutant. Hybridization of labeled cDNA to a macroarray of 145 PCR-amplified *D. vulgaris* genes encoding proteins active in energy metabolism indicated that the *adh* gene was among the most highly expressed in wild-type cells grown in LS medium. Relative to the wild type, expression of the *adh* gene was strongly downregulated in the *hyd* mutant, in agreement with the proteomic data. Expression was upregulated in ethanol-grown wild-type cells. An *adh* mutant was constructed and found to be incapable of growth in media in which ethanol was both the carbon source and electron donor for sulfate reduction or was only the carbon source, with hydrogen serving as electron donor. The *hyd* mutant also grew poorly on ethanol, in agreement with its low level of *adh* gene expression. The *adh* mutant grew to a lower final cell density on LS medium than the wild type. These results, as well as the high level of expression of *adh* in wild-type cells on media in which lactate, pyruvate, formate, or hydrogen served as the sole electron donor for sulfate reduction, indicate that ORF2977 Adh contributes to the energy metabolism of *D. vulgaris* under a wide variety of metabolic conditions. A hydrogen cycling mechanism is proposed in which protons and electrons originating from cytoplasmic ethanol oxidation by ORF2977 Adh are converted to hydrogen or hydrogen equivalents, possibly by a putative H_2-heterodisulfide oxidoreductase complex, which is then oxidized by periplasmic Fe-only hydrogenase to generate a proton gradient.

The role of the cytoplasmic membrane in the conservation of chemiosmotic energy is fairly well understood for aerobic bacteria, because of similarities to the mitochondrial inner membrane paradigm. However, this role is much less clear for anaerobes. For instance, chemiosmotic energy conservation is crucial for sulfate-reducing bacteria (SRB), when growing with lactate as the electron donor, because the ATP yield of substrate-level phosphorylation exactly balances what is required for sulfate activation (19, 21, 33). Odom and Peck proposed that SRB of the genus *Desulfovibrio* conserve chemiosmotic energy by hydrogen cycling (17). In their model, hydrogen generated from cytoplasmic lactate oxidation was proposed to diffuse across the cytoplasmic membrane, where it is oxidized by periplasmic hydrogenase to form a proton gradient with the electrons being conducted back to the cytoplasmic sulfate reduction pathway. Analysis of the genome sequence for *Desulfovibrio vulgaris* Hildenborough (http://www.tigr.org) has indicated the presence of two cytoplasm-facing, membrane-bound hydrogenases, four periplasmic hydrogenases, and a variety of transmembrane electron-transporting complexes. Hence, all components required for a hydrogen cycling mechanism of energy conservation are present in *D. vulgaris*. However, detailed physiological analysis of mutants lacking either the *hyd* genes for periplasmic Fe-only hydrogenase or the *hmc* genes for the transmembrane, electron-transporting high-molecular-weight cytochrome (Hmc) complex has revealed a more complicated picture (5, 18, 30). Relative to the wild-type strain, the *hyd* mutant appeared to produce significant amounts of CO from pyruvate. CO was formed transiently in cultures containing lactate or pyruvate and excess sulfate (30), indicating that it was both produced and consumed. The genome sequence of *D. vulgaris* also indicates the presence of a cytoplasmic pyruvate-formate lyase and of multiple periplasmic formate dehydrogenases. Hence, cycling of metabolites other than hydrogen (i.e., CO and formate) may contribute to chemiosmotic energy conservation during sulfate reduction with lactate (30).

Because the *D. vulgaris* genome sequence is known, the question of which proteins are involved in chemiosmotic energy conservation can now be pursued by proteomic or functional genomic approaches. In view of the significant physiological differences between the *hyd* mutant and wild-type strain (30), we focused initial studies on a comparison of these two strains.

MATERIALS AND METHODS

Materials. Mixed gases (85% [vol/vol] N_2, 10% [vol/vol] CO_2, and 5% [vol/vol] H_2; as well as 90% [vol/vol] N_2 and 10% [vol/vol] CO_2) were obtained from Praxair Products, Inc., Edmonton, Alberta, Canada. Restriction enzymes, *Taq* polymerase, DNA ligase, and Hybond-N membranes were obtained from Amersham Pharmacia Biotech, Baie d'Urfe, Quebec, Canada, whereas Superscript

* Corresponding author. Mailing address: Department of Biological Sciences, University of Calgary, 2500 University Dr. NW, Calgary, Alberta T2N 1N4, Canada. Phone: 403-220-6388. Fax: 403-289-9311. E-mail: voordouw@ucalgary.ca.

TABLE 1. Bacterial strains, primers, vectors, and plasmids used

Strain, plasmid, or primer	Genotype, sequence (position), and/or comment(s)	Source or reference
Strains		
D. vulgaris subsp. *vulgaris* Hildenborough		
Wild type	NCIMB 8303; isolated from clay soil near Hildenborough, United Kingdom	19
Hyd100	Δ*hydA,B;* Cm^r	18
ADH100	Δ*adh;* Cm^r	This study
ADH8	pNotΔAdhCmMob integrated into the chromosome; Suc^s Cm^r	This study
E. coli S17-1	*thi pro hsdR hsdM*$^+$ *recA* RP4-2 (Tc::Mu, Km::Tn*7*)	25
Plasmids		
pUC19Cm	pUC19 containing the *cat* gene	7
pNOT19	Cloning vector pUC19; *Nde*I site replaced by a *Not*I site	24
pMOB2	Contains *oriT* of plasmid RP4 and *Bacillus subtilis sacBR* genes on a 4.5-kb *Not*I fragment; Km^r Cm^r	24
pNotAdh, pNotΔAdh, pNotΔAdhBam, pNotΔAdhCmMob		This study (see text)
Primers		
P206-f	5′-cccggtaCCATGCTTCAGGGGCTGAAGCCC (−581 to −560)[a]	
P207-r	5′-ACAACTGGAGCAGGACAGGC (1627 to 1647)[a]	

[a] Positions relative to the *adh* coding region (bp 1 to 1179). Lowercase letters in P206-f are bases added to create a *Kpn*I cleavage site.

II RNase H^- reverse transcriptase was obtained from Invitrogen, Burlington, Ontario, Canada. [α-^{32}P]dCTP (10 mCi/ml [3,000 Ci/mmol]) was purchased from ICN Biomedicals, Inc., Irvine, Calif. Reagent-grade chemicals were obtained from BDH, Fisher, or Sigma. RNeasy kits, RNAprotect reagent, and RNase-free DNase were purchased from Qiagen, Mississauga, Ontario, Canada. Deoxyoligonucleotide primers were obtained from University Core DNA Services of the University of Calgary.

Bacterial strains, plasmids, and primers. The strains and plasmids used in this study are listed in Table 1. The primers listed in Table 1 were used for construction of the *D. vulgaris adh* mutant. Sequences of 290 forward and reverse primers used to PCR amplify 145 genes involved in energy metabolism of *D. vulgaris* chosen from a preliminary annotation of the genome were designed with Primer 3 (www-genome.wi.mit.edu/cgi-bin/primer/primer3_www.cgi) to have a T_m of 60°C and were synthesized by University Core DNA Services with a 96-well MerMade IV system from Bioautomation (Plano, Tex.). The sequences used have been listed elsewhere (www.ucalgary.ca/SC/BI/divisions/cmmb/voordouw2.html).

Growth of bacteria. For construction of the *adh* mutant, *Escherichia coli* and *D. vulgaris* strains were cultured in media described elsewhere (7, 18). For proteomic and gene array analyses, *D. vulgaris* wild-type or mutant strains were grown in Widdel Pfennig (WP) medium formulated according to Widdel and Bak (34) under an anoxic atmosphere of 90% N_2–10% CO_2 (vol/vol). WP-LS medium contained 38 mM lactate and 28 mM sulfate. Pyruvate (30 mM), formate (70 mM), and ethanol (40 mM) were used as alternative organic electron donors. Cultures in WP medium with hydrogen as the electron donor were in a mixed gas atmosphere (85% [vol/vol] N_2, 10% [vol/vol] CO_2, 5% [vol/vol] H_2) with either CO_2 and 3 mM acetate or CO_2 and 3 mM ethanol as the carbon source. The optical density of cultures at 600 nm (OD_{600}) was determined with a Shimadzu UV-visible spectrophotometer. Sulfate and sulfide concentrations were determined as described elsewhere (15).

2DE. Cultures (50 to 250 ml) in WP-LS medium were harvested in the mid-exponential phase (OD_{600} = 0.3). Following harvesting of cells by centrifugation (10,000 × *g*, 20 min, 4°C), Tris-EDTA (TE) extracts were prepared by resuspending the pellets in 0.1 M Tris–0.1 M EDTA (pH 9) equivalent to 0.01 $V \times OD_{600}$, where V is the volume (milliliters) and OD_{600} is the OD of the culture at the time of harvesting and processing as described elsewhere (6). Aliquots (50 μl) of TE extracts were frozen in liquid nitrogen and stored at −80°C. TE extracts had a protein content of 3.1 to 5.4 mg/ml, as determined by the method of Bradford (2). Isoelectric focusing was carried out with the IPGphor system using 18-cm strips with immobilized pH gradients (IPGs) of 3 to 10 nonlinear (NL), 4 to 7, and 6 to 9 (Amersham Biosciences, Freiburg, Germany). For silver and colloidal Coomassie brilliant blue (cCBB) staining, 20 to 40 μg and 50 to 200 μg of protein were loaded into the IPG strip holders, respectively. The appropriate volume of TE extract was diluted with rehydration buffer (8). Conditions for rehydration, sample entry, and isoelectric focusing were as described by Rabus et al. (20). After isoelectric focusing, the strips were incubated in equilibration buffer containing dithiothreitol (DTT) and then in equilibration buffer containing iodoacetamide (8, 20). Proteins were separated by two-dimensional gel electrophoresis (2DE) using an electrophoresis system from Genomic Solutions, Inc. (Ann Arbor, Mich.), as recently described (8, 20). Following electrophoresis, gels were fixed and stained with silver or cCBB (16). Data acquisition of stained gels was performed with the IMAGE scanner (Amersham Biosciences).

Amino acid and mass spectrometric analysis. Protein spots stained with cCBB were excised manually. Tryptic digest of proteins and separation of peptide fragments by high-performance liquid chromatography was carried out as described before (12). Determination of amino acid sequences by Edman-degradation (11) and of peptide masses by matrix-assisted laser desorption ionization–time of flight mass spectrometry (MALDI-TOF MS) (4) was carried out by TopLab (Martinsried, Germany). Protein identification and genome analysis were based on a preliminary list of annotated genes from the genomic sequence of *D. vulgaris*. Peptide mass fingerprints were mapped to the coding genes by using the MS-Digest program (3). For matching of experimentally determined peptide masses with theoretical values, differences of about 50 ppm were allowed as thresholds.

Design and production of a *D. vulgaris* macroarray. A set of 177 open reading frames (ORFs) encoding proteins involved in energy metabolism (for a complete list, see www.ucalgary.ca/SC/BI/divisions/cmmb/voordouw2.html) was identified from a preliminary annotation of the *D. vulgaris* genome. Primers for PCR amplification of this set covered as much of each ORF as possible. PCR products ranged in length from 0.1 to 2.9 kb. In some cases, two or more ORFs in the same operon were amplified together. PCRs (50 μl) included 5 μl of 10× PCR buffer (500 mM KCl, 15 mM $MgCl_2$, 100 mM Tris-HCl [pH 9]), 1 μl of deoxynucleoside triphosphates (dNTPs [2.5 mM each]), 1 μl of each primer (20 pmol/μl), 0.2 μl of *Taq* polymerase (5 U/μl), and either a large (100 ng) or small (1 ng) amount of *D. vulgaris* chromosomal DNA. Amplification was in a Perkin-Elmer GeneAmp 2400 PCR system by incubation for 5 min at 94°C, followed by 30 cycles of 30 s at 94°C; 30 s at 55°C; and 90, 120, or 180 s at 72°C, depending on the size of the expected product (up to 1 kb, 1 to 2 kb, or 2 to 3 kb, respectively). When using 100 ng of chromosomal DNA as the template, the product of the first PCR was diluted 500-fold, and 1 μl was used as the template in a second PCR. When using 1 ng of DNA, the product of the first PCR was used directly. PCR products were visualized on 0.7% (wt/vol) agarose gels stained with ethidium bromide. Those used for array construction (145 PCR products covering 159 of the 177

ORFs identified initially) consisted of single bands of the expected size. PCR products (25 to 100 ng/μl, as determined fluorimetrically) were incubated in a boiling water bath (3 min) and then in an ice bath (3 min). Aliquots (1 μl) of denatured PCR products were spotted 0.6 cm apart on Hybond-N membranes with a PB600 repeating dispenser (Hamilton, Co., Reno, Nevada), fitted with a 50-μl no. 710 Hamilton syringe. A PCR-negative control reaction mixture with 1 ng of chromosomal DNA but no primers was spotted as a negative control (0.02 ng of chromosomal DNA per spot). Bacteriophage λ DNA was also spotted as a negative control, whereas denatured *D. vulgaris* chromosomal DNA (12.5 to 1.6 ng per spot) was spotted as positive controls. After drying, DNAs were covalently linked to the arrays by UV irradiation. Macroarrays were stored at room temperature.

Hybridization with labeled cDNA. RNA was prepared from 50-ml cultures grown to half-maximal density in WP medium. One volume of culture was added to 2 volumes of Qiagen RNAprotect reagent, and RNA was extracted and purified with the Qiagen RNeasy kit with on-column DNase treatment. Samples of purified, DNA-free RNA in RNase-free water were stored at −80°C. Reverse transcription reaction mixtures (50 μl) contained 5 μg of RNA, 1 μl of random hexamers (0.25 μg/μl), 2.5 μl of dNTP mix (20 mM each dATP, dGTP, and dTTP), 200 U of reverse transcriptase, 100 μCi of [α-^{32}P]dCTP (3,000 Ci/mmol), 10 μl of 5× First Strand buffer (250 mM Tris-Cl [pH 8.3], 375 mM KCl, 15 mM $MgCl_2$), and 5 μl of 0.1 M DTT and were carried out according to the manufacturer's instructions. The RNA substrate was degraded by adding 50 μl of 0.27 M NaOH–20 mM EDTA and incubating this mixture at 65°C for 30 min. Reactions were neutralized by adding 50 μl of 1 M Tris-Cl (pH 7.4). RNA-free, chromosomal DNA of wild-type *D. vulgaris* (14) was labeled by using random hexamers (26, 32). Labeled cDNA or genomic DNA probes were hybridized to the arrays at 68°C by a high-stringency procedure (22, 31). After washing and drying, the arrays were exposed to BAS-IIIS type imaging plates for 4 h. These were scanned with a BAS1000 bio-imaging analyzer (Fuji). MacBas 2.2 software gave hybridization intensities in units of photostimulable luminescence (PSL) for all spots. Net values (ΔPSL) were obtained by subtracting negative control values, and the sum, ΣΔPSL, of all 145 ΔPSL values was calculated. ΔPSL_S values were calculated as $(\Delta PSL/\Sigma\Delta PSL) \cdot 100$. On average, ΔPSL_S values differed by 4.5% from the mean in duplicate experiments in which a labeled cDNA from the same mRNA pool was split and hybridized to two macroarrays. ΔPSL_S values obtained for labeled cDNAs from independently prepared mRNA pools differed on average by 16.9% from the mean. Average ΔPSL_S values were calculated for four array hybridizations by using labeled cDNAs from two independently prepared RNA samples hybridized in duplicate. Average values for ΔPSL_S were divided by average values obtained with the genomic DNA probe to obtain net relative hybridization intensities (I_R), corrected for different concentrations of the immobilized target gene, as well as for differences in signal intensity due to the different lengths of the PCR products.

Construction of the *adh* mutant. The gene for ORF2977 Adh, flanked by 500-bp upstream and downstream regions, was amplified with primers P206-f and P207-r (Table 1), cut with *Kpn*I and *Pst*I, and cloned in pNOT19 to give pNotAdh. Cleavage with *Sal*I and ligation gave pNotΔAdh, in which bp 387 to 502 of the 1,179-bp *adh* coding region were deleted. Plasmids pNotΔAdhBam, pNotΔAdhCm, and pNotΔAdhCmMob were created by sequential insertion of (i) a *Sal*I-*Bam*HI adapter (5′-TCGAGGGATCCC), (ii) the 1.4-kb *Bam*HI fragment from pUC19Cm containing the *cat* gene, and (iii) the 4.2-kb *Not*I fragment from pMOB2 containing *oriT* and *sacB*. The suicide plasmid was transferred to *D. vulgaris* by conjugation with *E. coli* S17-1 (pNotΔAdhCmMob). A single-crossover integrant, *D. vulgaris* ADH11, in which pNotΔAdhCmMob had integrated through the upstream homologous regions, was selected. Computer analysis indicated that Southern blotting of *Sal*I-digested chromosomal DNAs, using the labeled wild-type P206-f and P207-r amplicon as the probe, would give distinctly sized hybridizing fragments for the wild type (1.7 and 2.3 kb), the integrant (1.3, 2.3, and 8.3 kb), and the double-crossover deletion mutant (5.4 kb). Growth of *D. vulgaris* ADH11 in the presence of sucrose and chloramphenicol followed by colony purification gave *D. vulgaris* ADH100 with this expected Southern blot pattern (results not shown).

RESULTS

2DE. The protein compositions of TE extracts of the wild-type and *hyd* mutant *D. vulgaris* strains were compared by using IPG strips with IPGs of 3 to 10, 4 to 7, or 6 to 9 in the first dimension. The largest number of distinct protein spots was resolved with a pH gradient of 4 to 7 (Fig. 1). Twenty-nine prominent proteins were excised from cCBB-stained 2DE gels and identified by MALDI-TOF analysis of trypsin digests (Table 2). Their positions in silver-stained gels are indicated in Fig. 1 and 2. Their theoretical molecular masses agreed well with their positions on the gel, except for spots 3 to 7, 12, and 14. Spots 4 and 5 were identified as a 94.1-kDa membrane-protein that would not be expected in the TE extract, unless the observed mass (32 kDa) represents a smaller, soluble fragment. As reported before (6), the TE extract contains both periplasmic and cytoplasmic proteins, even though this extraction method was thought to specifically extract periplasmic proteins (29). Although periplasmic proteins were present (Table 2), most of the identified proteins were cytoplasmic. This included EF-Ts and EF-Tu (Fig. 1, spots 13 and 20), elongation factors in protein synthesis that are among the most highly expressed proteins in growing bacterial cells. A protein typical for anaerobic energy metabolism was acetate kinase (Fig. 1, spot 25), whereas an enzyme typical for sulfate reducers, sulfate adenylyltransferase (ATP sulfurylase), was represented by spots 16 and 17, indicating posttranslational processing. Nigerythrin, which has an oxygen defense function, was also identified (Fig. 1, spot 11). The TE extract thus contains a wide variety of soluble cytoplasmic and periplasmic proteins. Comparison of more than 10 2DE gels indicated that TE extraction represents an easy and reproducible way to characterize the *D. vulgaris* proteome.

Despite the significant physiological differences between wild-type and *hyd* mutant *D. vulgaris* (30), it appeared that the proteomes of WP-LS-grown cells were quite similar (Fig. 1). Significant differences were only seen in spot 1, resolved in spots 1a and 1b when a pH gradient of 6 to 9 was used (Fig. 2). These were seen in the wild type but not in the *hyd* mutant, whereas spots 2 and 3 were more prominent in the *hyd* mutant than in the wild-type proteome. Because of its similar molecular mass, spot 1 was thought to represent the 46-kDa α-subunit of Fe-only hydrogenase (HydA), which is absent from the TE extract of the *hyd* mutant as judged by immunoblotting (18). However, MALDI-TOF analysis of trypsin digests indicated that spots 1a and 1b both represent ORF2977 Adh, not HydA. This was confirmed by Edman degradation analysis, which indicated AVQEQVYGFFIPR as the N terminus for both spots, matching that predicted for ORF2977 Adh. The presence of two spots with the same M_r, but distinct pIs, indicates posttranslational modification of ORF2977 Adh. HydA was not identified either on 2DE gels with different IPGs or with protein blotting of a wide-pH-range gel, indicating its loss during isoelectric focusing. Proteins 2 and 3, which appeared more abundant in the *hyd* mutant than in the wild type, did not have a function associated with hydrogen metabolism (Table 2). Both were more abundant in the wild-type strain during the stationary phase (not shown). The more sluggish growth of the *hyd* mutant on WP-LS medium (30) may have caused higher abundance of these proteins to occur earlier. In contrast, the absence of spots 1 in the *hyd* mutant was a constant feature. Thus the main difference in the two proteomes is a near absence of ORF2977 Adh in the *hyd* mutant, as compared to the wild type.

Gene arrays. The pattern resulting from hybridization of labeled cDNA prepared from WP-LS grown wild-type *D. vulgaris* RNA to a macroarray is shown in Fig. 3A. I_R values for all

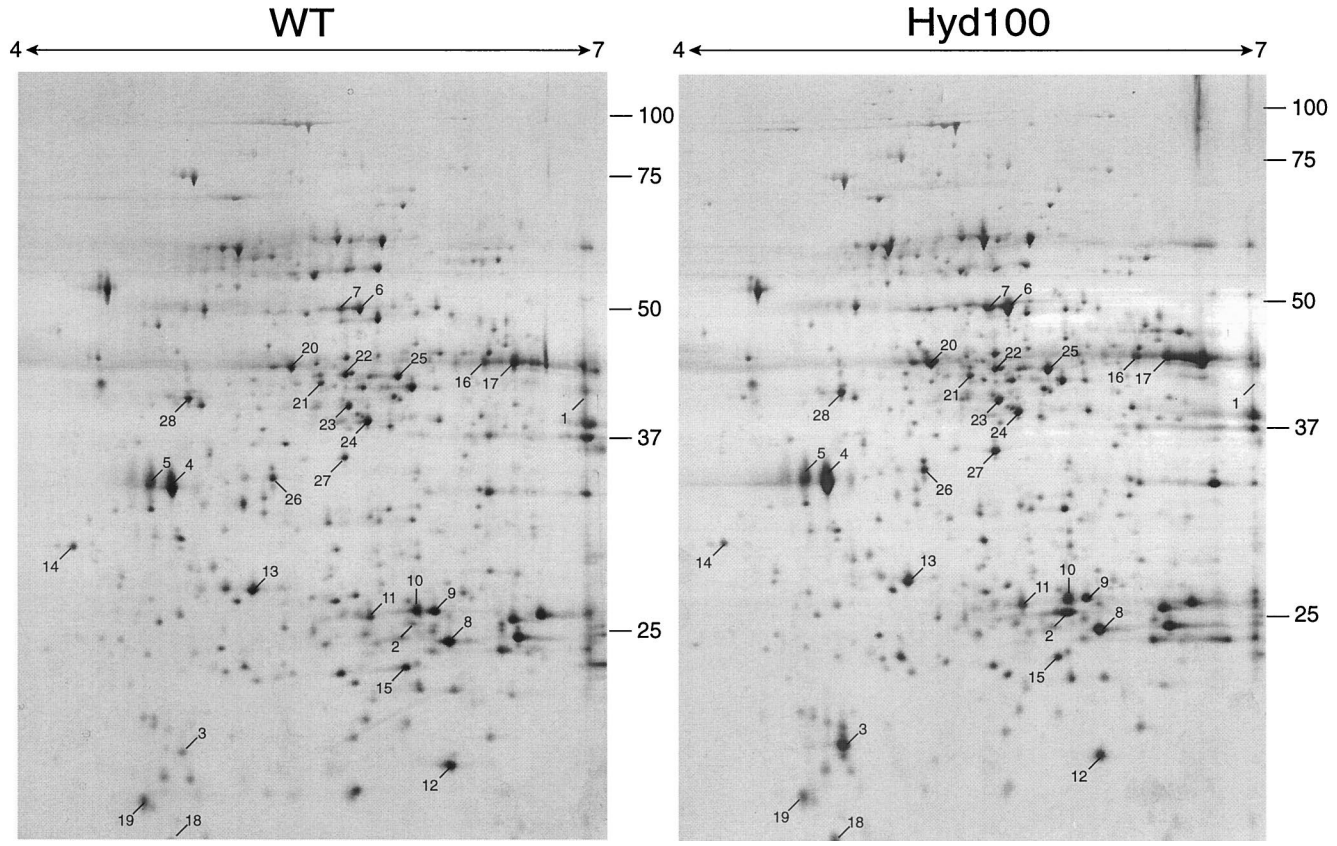

FIG. 1. Silver-stained 2DE gels of TE extracts from *D. vulgaris* wild-type (WT) and *hyd* mutant (Hyd100) strains. Proteins were separated by isoelectric focusing with IPGs of 4 to 7, as indicated. All numerically marked spots were identified by MALDI-TOF-MS (Table 2). Protein 1 is at the right edge of this pH gradient.

array results are listed at www.ucalgary.ca/SC/BI/divisions/cmmb/voordouw2.html. The reproducibility of macroarray hybridizations for RNA samples extracted from two separate cultures of the wild type in WP-LS is shown in Fig. 4A. All data points fall within a corridor that represents a fourfold change in RNA expression. Hence, gene expression changes within this fourfold corridor may not be significant. Under these conditions, the most highly expressed genes encode proteins involved in sulfate reduction (*sat*, *apsBA*, *dsrABD*, *dsrC*, and *ppaC*), lactate oxidation (*por* and *ack*), ethanol oxidation (*adh*), electron transport in the periplasm (*cyc*) and across the cytoplasmic membrane (*thcE*), ATP synthesis (*atpA* and *atpD*), and oxygen resistance (*sor* and *rub*) (Table 3). Interestingly, ORF2977 *adh* was the most highly expressed of the set of 145 genes represented on the macroarray. Expression of ORF2977 *adh* was further increased in wild-type cells grown with ethanol, but significantly decreased in the *hyd* mutant (Fig. 3B and C). A comparison of array data for the *hyd* mutant and wild type is shown in Fig. 4B. Spots outside the fourfold corridor were ORF2977 *adh*, ORF2976 and ORF2967, putative H_2-heterodisulfide reductase complex subunits (Fig. 4B, spots 1 to 3, downregulated), as well as ORF2128-2130 *hynAB* NiFe hydrogenase and an ORF3201-encoded hybrid cluster protein of unknown function (Fig. 4B, spots 4 and 5, upregulated). The ORF2976 and ORF2967 putative H_2-Hdr complex was also downregulated in the *adh* mutant in addition to ORF3423 flavodoxin, whereas ORF2437 carbon monoxide dehydrogenase was upregulated (data not shown). In the *hyd* mutant, *hydAB* gave no significant hybridization signal, in agreement with the fact that the *hydAB* genes were completely deleted (18). There was a residual *adh* message signal in the *adh* mutant (Fig. 3D). Because only a portion of the *adh* gene was deleted, this likely represented the 5′ end of the *adh* gene. 2DE analysis of the *adh* mutant showed the absence of ORF2977 Adh as in Fig. 2 (data not shown).

Expression of the *adh* gene relative to that of the wild type grown in WP-LS is summarized in Table 4. Expression was found to be even higher for the wild type grown with ethanol (see also Fig. 3B) and to be low in the *hyd* mutant (Fig. 3C and Table 4). Although in wild-type cells, expression of *adh* depended somewhat on the choice of electron donor, it was one of the most highly expressed genes irrespective of whether lactate, pyruvate, formate, ethanol, or hydrogen was used (Table 4). The array data thus confirm the results of proteomic analysis in that *adh* expression is low in the *hyd* mutant.

Physiological analysis of the *adh* mutant. Despite the high level of expression of the *adh* gene, it was relatively easy to make a mutant, indicating that ORF2977 Adh is not essential to *D. vulgaris* when cells are grown with either lactate or hydrogen as the electron donor for sulfate reduction. Growth in WP-LS medium (lactate as the electron donor) is compared in Fig. 5A and B. Although the *adh* mutant appeared to grow well

TABLE 2. Mass spectrometric identification of proteins from *D. vulgaris* separated by 2DE

Spot no.[a]	ID[b]	Sequence coverage (%)[c]	Significance[d]	pI[e]	M_r[f]	Location[g]	Possible function (gene)[h]
1a	ORF02977	32	5.8 e-22	6.8	41.8	C	Alcohol dehydrogenase
1b	ORF02977	44	5.7 e-27	6.8	41.8	C	Alcohol dehydrogenase
2	ORF03570	26	3.0 e-06	6.0	28.5	P	Conserved hypothetical protein (periplasmic)
3	ORF04254	13	1.5 e-04	6.7	28.4*	C	Ubiquinone/menaquinone biosynthesis methyltransferase (*ubiE*)
4	ORF02836	68	6.5 e-50	5.1	94.1*	M	Cation-transporting ATPase, E1-E2 family
5	ORF02836	58	2.0 e-37	5.1	94.1*	M	Cation-transporting ATPase, E1-E2 family
6	ORF00572	40	1.9 e-31	4.7	87.1*	C	PTS system, fructose-specific EIIA/HPr/EI components (*ptsI*)
7	ORF00572	41	7.7 e-39	4.7	87.1*	C	PTS system, fructose-specific EIIA/HPr/EI components (*ptsI*)
8	ORF00988	63	1.4 e-29	5.8	26.8	P	Arginine ABC transporter, periplasmic arginine-binding protein, putative
9	ORF02865	52	1.3 e-19	7.0	29.7	P	Amino acid ABC transporter, amino acid-binding protein, putative
10	ORF00176	32	2.1 e-14	7.1	30.4	P	Amino acid ABC transporter, amino acid-binding protein, putative
11	ORF04661	42	1.1 e-19	4.9	20.2	C	Nigerythrin
12	ORF04056	9	2.2 e-04	5.7	63.5*	C	Sensory box/GGDEF family protein
13	ORF00383	56	4.6 e-29	5.0	30.5	C	Translation elongation factor Ts (*tsf*)
14	ORF00347	54	5.6 e-18	4.9	20.2*	C	Hypothetical protein
15	ORF00590	57	1.4 e-23	5.4	21.2	C	ThiJ/PfpI family superfamily
16	ORF01081	45	2.8 e-37	6.0	47.5	C	Sulfate adenylyltransferase (*sat*)
17	ORF01081	52	1.7 e-41	6.0	47.5	C	Sulfate adenylyltransferase (*sat*)
18	ORF03883	69	3.4 e-17	5.4	17.0	C	Nitrogen assimilation regulatory protein (*Klebsiella,* putative)
19	ORF02097	42	2.4 e-13	4.6	17.7	C	Purine-binding chemotaxis protein CheW (*cheW-1*)
20	ORF03811	43	5.9 e-25	4.8	43.4	C	Translation elongation factor Tu (*tuf*)
21	ORF03178	60	1.6 e-36	5.1	41.4	C	Phosphoglycerate kinases
22	ORF03040	54	4.3 e-37	5.3	42.4	C	*S*-Adenosylmethionine synthetase (*metK*)
23	ORF01685	46	6.5 e-45	5.2	42.7	C	Aminotransferase, class I (*aspC4*)
24	ORF04028	42	3.6 e-30	5.2	38.3	C	Aspartate-semialdehyde dehydrogenase (*asd*)
25	ORF03996	54	1.3 e-37	5.8	36.7	C	Acetate kinase (*ackA*)
26	ORF05210	26	5.1 e-20	4.9	28.9	C	3-Deoxy-D-manno-octulosonate cytidylyltransferase (*kdsB*)
27	ORF04793	58	2.3 e-35	5.5	38.9	P	Periplasmic spermidine/putrescine-binding protein (*potD-1*)
28	ORF00568	52	3.8 e-42	5.2	38.1	C	Dihydroxyacetone kinase family protein (*b1200*)

[a] Spot numbers in 2DE gels shown in Fig. 1 and 2.
[b] Identification by mass spectrometry in a database of coding genes (http://www.tigr.org). Spots 1a and 1b were also identified by N-terminal sequence analysis.
[c] Extent to which the combined peptide masses cover the indicated sequence. Low coverage of proteins 3 and 12 was due to problems with mass spectrometry calibration and N-terminal truncation, respectively.
[d] Significance of the match between experimental and theoretical peptide masses as expressed by the probability that the match is due to random chance.
[e] pI is the average theoretical value calculated with programs found at http://www.embl-heidelberg.de/cgi/pi-wrapper.pl and http://www.biologie.uni-freiburg.de/data/PcIP.html.
[f] M_r is the theoretical molecular mass derived from the genome sequence. *, disagreement with M_r observed in Fig. 3.
[g] Most likely location—periplasmic (P), cytoplasmic (C), or in the membrane (M)—based on evaluation of the amino acid sequence.
[h] Annotated function.

in this medium, it reached a lower final cell density: OD_{600} = 0.420 ± 0.015 and 0.475 ± 0.019 for the *adh* mutant and wild-type strains, respectively (mean of five determinations). This indicates that, although not essential, ORF2977 Adh contributes to the bioenergetics of *D. vulgaris* during growth on lactate-containing medium. The *hyd* mutant also grew to lower final cell density compared to the wild type (OD_{600} = 0.435 ± 0.032) in WP-LS medium.

When using ethanol as a carbon source and electron donor, no sulfate reduction and associated growth was seen for the

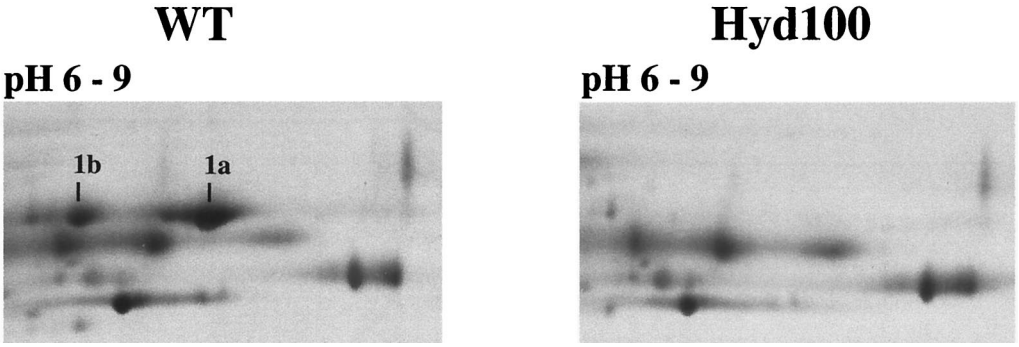

FIG. 2. Silver-stained 2DE gels of TE extracts from *D. vulgaris* wild-type (WT) and *hyd* mutant (Hyd100) strains. Proteins were separated by isoelectric focusing with IPGs of 6 to 9. Proteins 1a and 1b were identified by MALDI-TOF-MS and Edman degradation. Only a portion of each gel is shown.

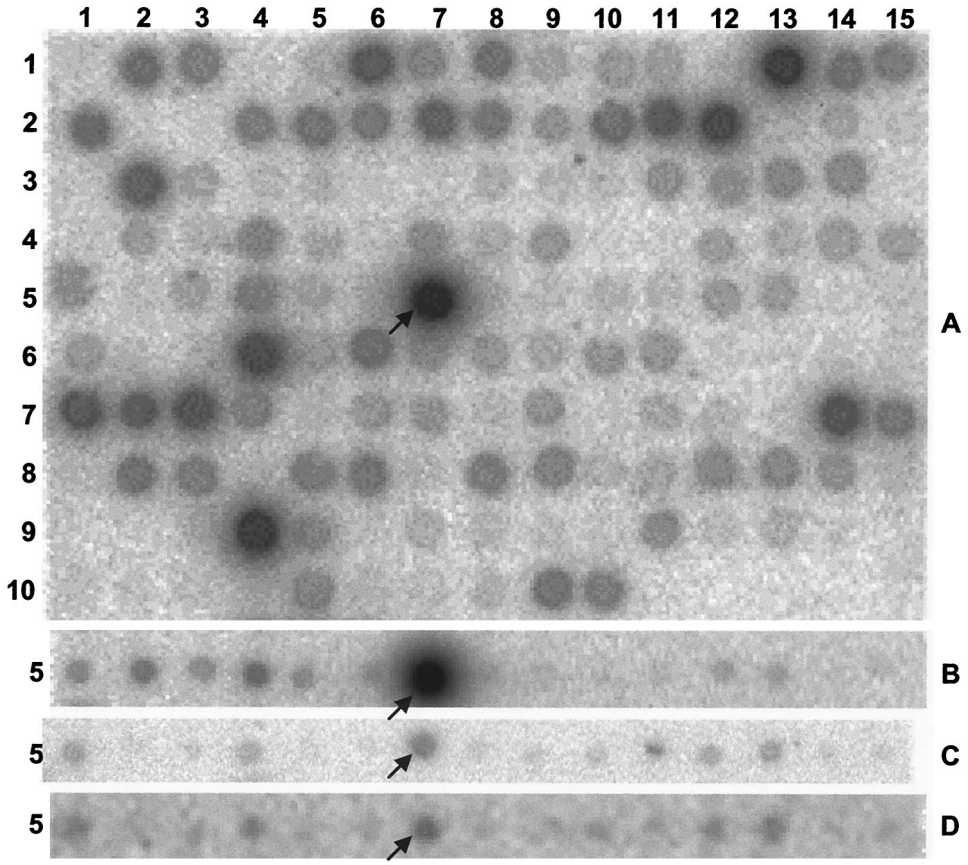

FIG. 3. Hybridization of *D. vulgaris* macroarrays with labeled cDNA synthesized in vitro. (A) RNA extracted from wild-type cells grown in WP-LS medium. The entire macroarray is shown (145 spots, 15 columns, 10 rows). (B) RNA extracted from wild-type cells grown in WP medium with ethanol as the sole electron donor. Only row 5 of the array is shown. (C) RNA extracted from *hyd* mutant cells grown in WP-LS medium. Only row 5 of the array is shown. (D) RNA extracted from *adh* mutant cells grown in WP-LS medium. Only row 5 of the array is shown. The location of ORF2977 *adh* is indicated by an arrow. The array positions of other highly expressed genes are indicated in Table 3.

adh mutant, whereas the wild type reached a final cell density (OD_{600}) of 0.335 ± 0.012, as shown in Fig. 5C and D. The same result was obtained for cultures with 5% (vol/vol) H_2 as the electron donor and ethanol (and CO_2) as the carbon source (results not shown). Hence, despite the fact that the genome sequence indicates the presence of multiple ORFs that are annotated as "alcohol dehydrogenase," ORF2977 Adh appears to be the only enzyme catalyzing ethanol oxidation. The *hyd* mutant reached a final cell density (OD_{600}) of 0.248 ± 0.013 with ethanol as the carbon source and electron donor. Cultures of the *hyd* mutant transferred from WP-LS medium to WP medium with ethanol as the carbon source and electron donor had a lag phase of 200 to 250 h. Ethanol-grown cultures of the *hyd* mutant transferred to ethanol-containing media started to grow within 24 h.

DISCUSSION

The power of proteomics, functional genomics, or other molecular biology techniques for identification of proteins that function in energy metabolism of anaerobes has already been demonstrated. Schut et al. (23) identified genes involved in hydrogen metabolism and sulfur reduction from hybridization to a limited *Pyrococcus furiosus* microarray. Tersteegen and Hedderich (27) have shown by reverse transcription-PCR that two membrane-bound, energy-converting hydrogenases are induced in *Methanobacterium thermoautotrophicum* under hydrogen limitation, suggesting a role in energy conservation by some form of hydrogen cycling.

Our experiments point to an important role of ORF2977 Adh in the energy metabolism of *D. vulgaris*, which we wish to understand. Hensgens et al. (10) purified a close homolog of ORF2977 Adh from *D. gigas* cells grown on media containing ethanol and sulfate. The enzyme had a molecular mass of 43 kDa by sodium dodecyl sulfate-polyacrylamide gel electrophoresis (SDS-PAGE) (similar to ORF2977 Adh), assembled into decamers as judged by electron microscopy, and had a very similar N terminus, AVREQVYGFFIPSVTLIGIGA SKEI, compared to that for ORF2977 Adh, AVQEQVYG FFIPRVTLIGIGASKAI. Hensgens et al. (10) found this enzyme to be active towards ethanol, isopropanol, and a variety of other alcohols at lower activity. Because it was isolated from cells grown on ethanol, the authors concluded that catabolic oxidation of ethanol must be its primary function in *D. gigas*. We have confirmed here by mutation that ORF2977 Adh is the sole enzyme catalyzing ethanol oxidation in *D. vulgaris* (Fig. 5). Interestingly, it also functions during growth with lactate, pyru-

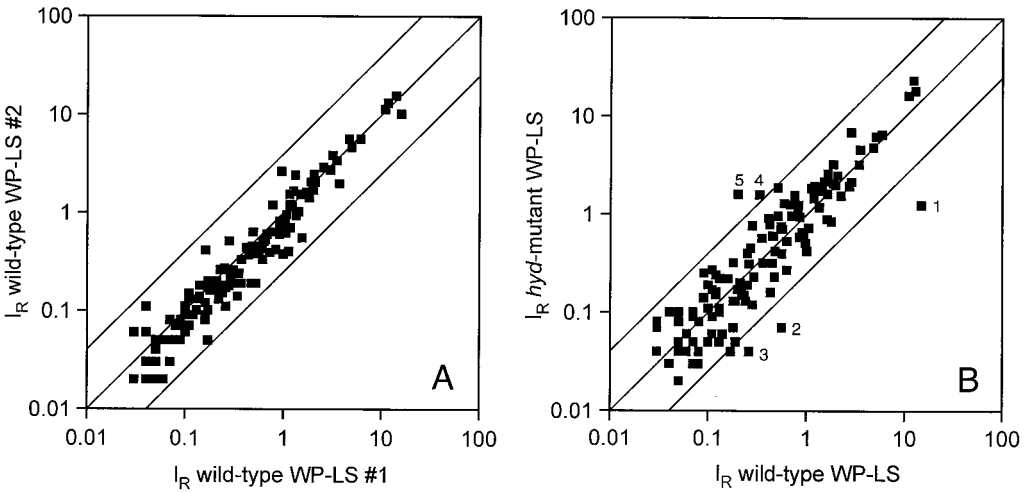

FIG. 4. Plots of relative hybridization intensities (I_R) for macroarray hybridizations of wild-type and *hyd* mutant *D. vulgaris* strains. The upper and lower lines represent a fourfold change in gene expression from the central line. (A) Comparison of RNA extracted from two separate cultures of the wild type in WP-LS medium. The data are means of two array hybridizations. (B) Comparison of gene expression for the wild type and *hyd* mutant grown in WP-LS. The data are means of four array hybridizations. Genes outside the fourfold expression corridor are as follows: 1, ORF2977 *adh*; 2, ORF2976 putative H_2:Hdr reductase complex subunit gene; 3, ORF2967 putative H_2:Hdr complex subunit gene; 4, ORF2128-2130 NiFe hydrogenase genes; and 5, ORF3201 hybrid cluster protein gene.

vate, formate, or hydrogen as an electron donor for sulfate reduction, because it is prominently expressed under all of these conditions (Table 4). The enzyme likely reoxidizes ethanol formed during metabolism of these different electron donors. For instance, *D. vulgaris* incompletely oxidizes lactate to acetate and CO_2 (21), and some of the acetate is converted to ethanol (28). The enzyme or enzymes forming the ethanol are currently unknown. With excess sulfate, ORF2977 Adh likely reoxidizes the ethanol formed later in the growth curve. Growth of *D. vulgaris* with hydrogen as the sole electron donor requires the presence of acetate as a carbon source. The need for ORF2977 Adh under these conditions can be understood when assuming that some of the acetate is transiently converted into ethanol.

Since ORF2977 Adh is a cytoplasmic enzyme, growth on ethanol as the sole electron donor for sulfate reduction requires some form of cycling of hydrogen (H_2) or hydrogen equivalents ([H]). The need for this is even more pressing than for growth on lactate (30), because oxidation of ethanol to acetate, the expected end product in *D. vulgaris*, does not yield ATP by substrate-level phosphorylation. Oxidation of 2 ethanol to 2 acetate per sulfate reduced, through the action of ORF2977 Adh and aldehyde dehydrogenase, yields 8 [H]. The proton gradient resulting from oxidation of 8 [H] by periplasmic hydrogenases can give sufficient ATP for the activation of sulfate prior to reduction (2 ATP per sulfate) and other metabolic processes (maximally 0.7 ATP per sulfate, assuming formation of 2.7 ATP per 8 H^+ by ATP synthase). The proteomic and functional genomic data collected in the present study shed some light on the mechanism by which the [H]

TABLE 3. Relative expression level (I_R) of the most highly expressed genes in a set of 145 represented on the macroarray[a]

ORF[b]	Gene	Description	I_R[c]	Position[d]
2977	*adh*	Alcohol dehydrogenase	14.8 ± 0.9	5, 7
3581	*dsrC*	Dissimilatory sulfite reductase	12.9 ± 2.8	6, 4
4250	*cyc*	Cytochrome c_3	12.3 ± 0.8	7, 14
336, 338	*apsBA*	APS reductase	11.0 ± 0.4	1, 13
5313, 5314, 5316	*dsrABD*	Dissimilatory sulfite reductase	5.9 ± 0.5	9, 4
219	*atpD*	ATP synthase F1 β-subunit	5.1 ± 0.5	1, 6
1081	*sat*	Sulfate adenylyltransferase	4.8 ± 0.2	2, 12
3986	*por*	Pyruvate:ferredoxin oxidoreductase	3.5 ± 0.3	7, 1
5316	*dsrD*	Dissimilatory sulfite reductase	3.4 ± 0.2	9, 5
4273	*rub*	Rubredoxin	2.9 ± 0.1	8, 1
4271	*sor*	Superoxide reductase	2.8 ± 0.9	7, 15
1642	*ppaC*	Pyrophosphatase	2.7 ± 0.2	3, 2
3996	*ack*	Acetate kinase	2.2 ± 0.2	7, 3
223	*atpA*	ATP Synthase F1 α-subunit	2.1 ± 0.1	1, 8
1072	*thcE*	Triheme cytochrome *c* operon membrane protein	2.0 ± 0.1	2, 11

[a] Macroarrays were hybridized with cDNA reverse transcribed from RNA extracted from wild-type *D. vulgaris* grown in WP-LS medium.
[b] ORF numbers in a preliminary annotation of the genome sequence (www.tigr.org).
[c] Calculated as indicated in the text. The mean of four determinations and the average deviation from the mean are shown.
[d] Position (row number, column number) of gene on the macroarray depicted in Fig. 3A.

TABLE 4. Relative expression level (I_R) of ORF2977 *adh* as determined by macroarray hybridization

Strain	Electron donor	I_R of *adh*[a]
Wild type	Lactate	14.8 ± 0.9
	Pyruvate	14.9 ± 5.0
	Ethanol	44.4 ± 5.5
	Formate	30.5 ± 5.2
	Hydrogen	34.6 ± 1.2
hyd mutant	Lactate	1.24 ± 0.3

[a] Calculated as indicated in the text. The mean of four determinations and the average deviation from the mean are shown.

liberated in ethanol oxidation are converted into a proton gradient.

Proteomic analysis indicated that deletion of the *hydAB* genes, encoding Fe-only hydrogenase (HydAB), significantly lowers the cellular content of ORF2977 Adh (Fig. 2). This result was confirmed by macroarray hybridizations in which transcription patterns of wild-type and *hyd* mutant *D. vulgaris* strains were compared (Fig. 4B, spot 1). Figure 4B also indicated downregulation of ORF2976 and ORF2967 putative H_2:Hdr complex (Fig. 4B, spots 2 and 3) and upregulation of ORF2128-2130 *hynAB* (Fig. 4B, spot 4) encoding NiFe-hydrogenase, possibly to compensate for the loss of HydAB. The ORF2976 and ORF2967 genes belong to a six-gene operon located 230 bp downstream of ORF2977 *adh*. The *adh* gene is not believed to be part of this operon, because the intergenic region is rather large and contains a putative hairpin loop. The operon consists of ORFs 2976, 2975, 2972, 2971, 2969, and 2967, encoding proteins predicted to be cytoplasmic. A BLAST search (1) showed that the closest homologs to ORFs 2976, 2975, and 2972 are subunits HdrC, HdrB, and HdrA of heterodisulfide reductase from *Carboxydothermus hydrogenovorans* or *M. thermoautotrophicum* (9). The closest homologs to ORF2971, -2969, and -2967 are the δ-, α-, and γ-subunits of (sulf)hydrogenase from *Pyrococcus*. The operon may thus encode a cytoplasmic heterodisulfide reductase-hydrogenase. Corresponding enzymes in methanogens are referred to as H_2-heterodisulfide oxidoreductase (H_2:Hdr). Macroarray analysis of the *adh* mutant also indicated downregulation of the genes encoding the ORF2976-2967 putative H_2:Hdr complex (data not shown). The close physical relationship and coexpression of ORF2977 *adh* and the operon for putative H_2:Hdr complex strongly suggest that [H] originating from ethanol oxidation are processed by H_2:Hdr.

In methanogens, a heterodisulfide of coenzymes M and B (CoM-S-S-CoB) and methane are formed in the final step of methanogenesis. Membrane-bound H_2:Hdr regenerates CoM-SH and CoB-SH by reduction of the heterodisulfide with hydrogen (9). This reaction is energy conserving and contributes to the proton motive force. The H_2:Hdr from *M. thermoautotrophicum* can be dissociated into a hydrogenase and a heterodisulfide reductase subcomplex, each consisting of three subunits (9). In addition to methanogens, heterodisulfide reductase homologs are found in the sulfate-reducing bacteria *D. vulgaris* and *D. desulfuricans*, in the sulfate-reducing archaeon *Archaeoglobus fulgidus* (13), in the metal-reducing bacterium *Geobacter metallireducens*, in the green sulfur bacterium *Chlorobium tepidum*, and in the CO-reducing bacterium *C. hydrogenoformans*, among others. The role of H_2:Hdr in nonmethanogens is unclear. In *D. vulgaris*, the ORF2976-2967 putative H_2:Hdr complex likely has a role in ethanol oxidation. A possible mechanism is that ORF2977 Adh transfers [H] from ethanol oxidation to a disulfide in H_2:Hdr, forming reduced enzyme (HS-E-SH), which is then converted to the oxidized form and H_2. In the hydrogen cycling hypothesis, this cytoplasmically generated H_2 diffuses to the periplasm, where it is oxidized by periplasmic hydrogenases (17). The latter model may be too simplistic, because it fails to explain why of several

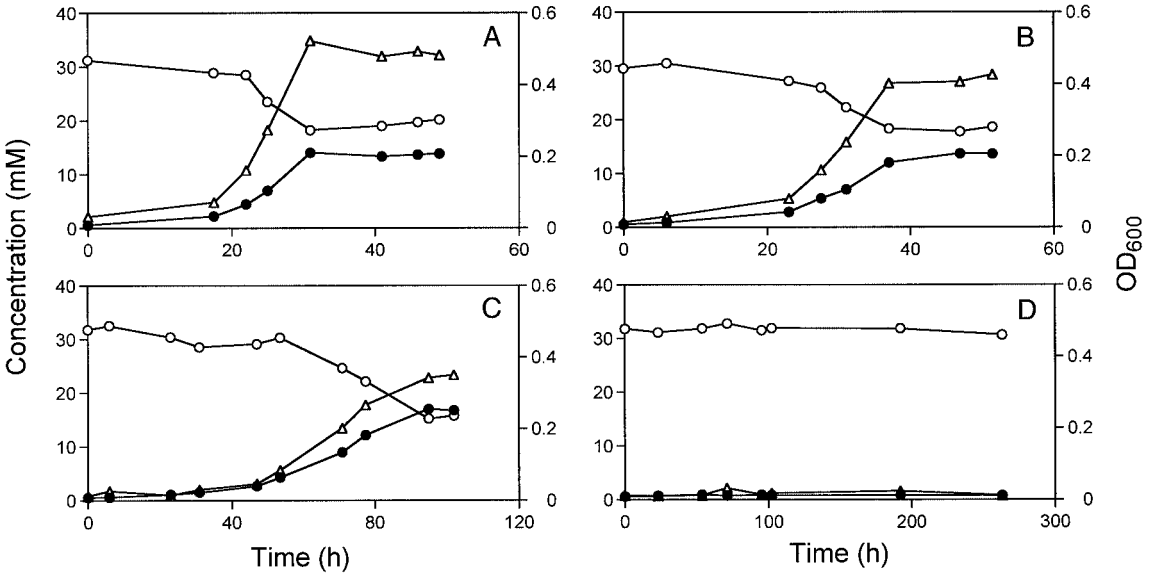

FIG. 5. Comparison of the growth physiologies of *D. vulgaris* wild-type and *adh* mutant strains. The cell density (△; OD_{600}, right ordinate), millimolar sulfate concentration (○; left ordinate), and millimolar sulfide concentration (●; left ordinate) are shown as a function of time. (A to D) Strains and electron donors. (A) Wild type with lactate. (B) *adh* mutant with lactate. (C) Wild type with ethanol. (D) *adh* mutant with ethanol.

periplasmic hydrogenases, HydAB is specifically required for ethanol oxidation. If H_2 were to diffuse freely, it could equally well be oxidized by any of three periplasmic NiFe-hydrogenases present in *D. vulgaris*. The specific requirement for HydAB suggests that the [H] formed in cytoplasmic ethanol oxidation by ORF2977 Adh are somehow transmitted through a specific chain involving cytoplasmic ORF2976-2967 H_2:Hdr and as yet unknown transmembrane components. Chemically the chain may consist of a number of linked H_2-disulfide oxidation-reduction events that eventually delivers 2 [H] as H_2 in the active site of periplasmic HydAB for final oxidation to protons. Oxidation of [H] originating from ethanol oxidation is not the only function of HydAB, as shown by physiological studies (18, 30) and by the fact that the HydAB content in the *adh* mutant is similar to that in the wild type as determined by immunoblotting (results not shown).

In summary, the proteomics, functional genomics, and gene mutation results obtained here further illustrate the complex transmembrane cycling mechanisms that conserve the free energy liberated when organic compounds are oxidized with sulfate in the sulfate-reducing bacteria.

ACKNOWLEDGMENTS

This work was supported by a Research Grant from the Natural Science and Engineering Research Council of Canada to G.V. and by the Max-Planck Society of Germany. G.V. acknowledges the support of a fellowship from the Hanse Wissenschaftskolleg in Bremen, Germany, and of a visiting professorship of the CNRS in Marseille, France. A database of the *D. vulgaris* Hildenborough genome was searched at the web site of The Institute for Genomic Research at http://www.tigr.org. Sequencing of this genome is financially supported by the U.S. Department of Energy.

We thank Richard Pon for synthesizing the oligonucleotides, Janine Wildschut and Daniela Lange for technical assistance, Thomas Halder for MS analysis, and Fritz Widdel for his interest in this work and many discussions.

REFERENCES

1. **Altschul, S. F., W. Gish, W. Miller, E. W. Myers, and D. J. Lipmann.** 1990. Basic local alignment search tool. J. Mol. Biol. **215:**403–410.
2. **Bradford, M. M.** 1976. A rapid and sensitive method for the quantitation of microgram quantities of protein utilizing the principle of protein-dye binding. Anal. Biochem. **72:**248–254.
3. **Clauser, K. R., P. Baker, and A. L. Burlingame.** 1999. Role of accurate mass measurement (±10 ppm) in protein identification strategies employing MS or MS/MS and database searching. Anal. Chem. **71:**2871–2882.
4. **Corthals, G. L., S. P. Gygi, R. Aebersold, and S. D. Patterson.** 2000. Identification of proteins by mass spectrometry, p. 197–231. *In* T. Rabilloud (ed.), Proteome research: two-dimensional gel electrophoresis and identification methods. Springer, Berlin, Germany.
5. **Dolla, A., B. K. J. Pohorelic, J. K. Voordouw, and G. Voordouw.** 2000. Deletion of the *hmc*-operon of *Desulfovibrio vulgaris* subsp. *vulgaris* Hildenborough hampers hydrogen metabolism and low-redox potential niche establishment. Arch. Microbiol. **174:**143–151.
6. **Fournier, M., Y. Zhang, J. D. Wildschut, A. Dolla, J. K. Voordouw, D. C. Schriemer, and G. Voordouw.** 2003. Function of oxygen resistance proteins in the anaerobic sulfate-reducing bacterium *Desulfovibrio vulgaris* Hildenborough. J. Bacteriol. **185:**71–79.
7. **Fu, R., and G. Voordouw.** 1997. Targeted gene replacement mutagenesis of *dcrA*, encoding an oxygen sensor of the sulfate-reducing bacterium *Desulfovibrio vulgaris* Hildenborough. Microbiology **143:**1815–1826.
8. **Görg, A., C. Obermaier, G. Boguth, A. Harder, B. Scheibe, R. Wildgruber, and W. Weiss.** 2000. The current state of two-dimensional electrophoresis with immobilized pH gradients. Electrophoresis **21:**1037–1053.
9. **Hedderich, R., J. Koch, D. Linder, and R. K. Thauer.** 1994. The heterodisulfide reductase from *Methanobacterium thermoautotrophicum* contains sequence motifs characteristic of pyridine-nucleotide-dependent thoredoxin reductases. Eur. J. Biochem. **225:**253–261.
10. **Hensgens, C. M. H., J. Vonck, J. van Beeumen, E. F. J. van Bruggen, and T. A. Hansen.** 1993. Purification and characterization of an oxygen-labile NAD-dependent alcohol dehydrogenase from *Desulfovibrio gigas*. J. Bacteriol. **175:**2859–2863.
11. **Hunkapillar, M. W., R. M. Hewick, J. M. Dreyer, and L. E. Hood.** 1983. High-sensitivity sequencing with a gas-phase sequenator. Methods Enzymol. **91:**399–413.
12. **Jenö, P., T. Mini, S. Moes, E. Hintermann, and M. Horst.** 1995. Internal sequences from proteins digested in polyacrylamide gels. Anal. Biochem. **224:**75–82.
13. **Mander, G. J., E. C. Duin, D. Linder, K. O. Stetter, and R. Hedderich.** 2002. Purification and characterization of a membrane-bound enzyme complex from the sulfate-reducing archaeon *Archaeoglobus fulgidus* related to heterodisulfide reductase from methanogenic archaea. Eur. J. Biochem. **269:** 1895–1904.
14. **Marmur, J.** 1961. A procedure for the isolation of deoxyribonucleic acid from micro-organisms. J. Mol. Biol. **3:**208–218.
15. **Nemati, M., T. J. Mazutinec, G. E. Jenneman, and G. Voordouw.** 2001. Control of biogenic H_2S production with nitrite and molybdate. J. Ind. Microbiol. Biotechnol. **26:**350–355.
16. **Neuhoff, V., R. Stamm, I. Pardowitz, N. Arold, W. Ehrhardt, and D. Taube.** 1990. Essential problems in quantification of proteins following colloidal staining with Coomassie brilliant blue dyes in polyacrylamide gels, and their solution. Electrophoresis **11:**101–117.
17. **Odom, J. M., and H. D. Peck, Jr.** 1981. Hydrogen cycling as a general mechanism for energy coupling in the sulfate-reducing bacteria *Desulfovibrio* sp. FEMS Microbiol. Lett. **12:**47–50.
18. **Pohorelic, B. K. J., J. K. Voordouw, E. Lojou, A. Dolla, J. Harder, and G. Voordouw.** 2002. Effects of deletion of genes encoding Fe-only hydrogenase of *Desulfovibrio vulgaris* Hildenborough on hydrogen and lactate metabolism. J. Bacteriol. **184:**679–686.
19. **Postgate, J. R.** 1984. The sulphate-reducing bacteria, 2nd ed. Cambridge University Press, Cambridge, United Kingdom.
20. **Rabus, R., D. Gade, R. Helbig, M. Bauer, F. O. Glöckner, M. Kube, H. Schlesner, R. Reinhardt, and R. Amann.** 2002. Analysis of *N*-acetylglucosamine metabolism in the marine bacterium *Pirellula* sp. strain 1 by a proteomic approach. Proteomics **2:**649–655.
21. **Rabus, R., T. Hansen, and F. Widdel.** 2001. Dissimilatory sulfate-and sulfur-reducing prokaryotes. *In* M. Dworkin, S. Falkow, E. Rosenberg, K.-H. Schleifer, and E. Stackebrandt (ed.), The prokaryotes: an evolving electronic resource for the microbiological community. [Online.] Springer Science Online, Heidelberg, Germany. www.prokaryotes.com.
22. **Sambrook, J., E. F. Fritsch, and T. Maniatis.** 1989. Molecular cloning: a laboratory manual, 2nd ed. Cold Spring Harbor Laboratory Press, Cold Spring Harbor, N.Y.
23. **Schut, G. J., J. Zhou, and M. W. W. Adams.** 2001. DNA microarray analysis of the hyperthermophilic archaeon *Pyrococcus furiosus*: evidence for a new type of sulfur-reducing enzyme complex. J. Bacteriol. **183:**7027–7036.
24. **Schweizer, H. P.** 1992. Allelic exchange in *Pseudomonas aeruginosa* using novel ColE1-type vectors and a family of cassettes containing a portable *oriT* and the counter-selectable *Bacillus subtilis sacB* marker. Mol. Microbiol. **6:**1195–1204.
25. **Simon, R., U. Priefer, and A. Pühler.** 1983. A broad-host-range mobilization system for *in vivo* genetic engineering: transposon mutagenesis in gram negative bacteria. Bio/Technology **1:**784–791.
26. **Telang, A. J., S. Ebert, J. M. Foght, D. W. S. Westlake, G. E. Jenneman, D. Gevertz, and G. Voordouw.** 1997. Effect of nitrate injection on the microbial community in an oil field as monitored by reverse sample genome probing. Appl. Environ. Microbiol. **63:**1785–1793.
27. **Tersteegen, A., and R. Hedderich.** 1999. *Methanobacterium thermoautotrophicum* encodes two multisubunit membrane-bound [NiFe] hydrogenases. Eur. J. Biochem. **264:**930–943.
28. **Traore, A. S., C. E. Hatchikian, J. P. Belaich, and J. Le Gall.** 1981. Microcalorimetric studies of the growth of sulfate-reducing bacteria: energetics of *Desulfovibrio vulgaris* growth. J. Bacteriol. **145:**191–199.
29. **van der Westen, H. M., S. G. Mayhhew, and C. Veeger.** 1978. Separation of hydrogenase from intact cells of *Desulfovibrio vulgaris*. FEBS Lett. **86:**122–126.
30. **Voordouw, G.** 2002. Carbon monoxide cycling by *Desulfovibrio vulgaris* Hildenborough. J. Bacteriol. **184:**5903–5911.
31. **Voordouw, G., J. D. Strang, and F. R. Wilson.** 1989. Organization of genes encoding [Fe] hydrogenase in *Desulfovibrio vulgaris* subsp. *oxamicus* Monticello. J. Bacteriol. **171:**3881–3889.
32. **Voordouw, G., J. K. Voordouw, T. R. Jack, J. Foght, P. M. Fedorak, and D. W. S. Westlake.** 1992. Identification of distinct communities of sulfate-reducing bacteria in oil fields by reverse sample genome probing. Appl. Environ. Microbiol. **58:**3542–3552.
33. **White, D.** 2000. The physiology and biochemistry of prokaryotes, 2nd ed., p. 318. Oxford University Press, New York, N.Y.
34. **Widdel, F., and F. Bak.** 1992. Gram-negative mesophilic sulfate-reducing bacteria, p. 3352–3378. *In* A. Balows, H. G. Truper, M. Dworkin, W. Harder, and K. H. Schleifer (ed.), The prokaryotes, 2nd ed., vol. 4. Springer-Verlag, New York, N.Y.